

# Comparison of the NIST High Accuracy Cryogenic Radiometer and the NIST Scale of Detector Spectral Response

*J. M. Houston, C. L. Cromer, J. E. Hardis  
and T. C. Larason*

**Abstract.** Two independent methods of measurement were used to determine the absolute spectral responsivity and external quantum efficiency of light-trapping silicon photodiode packages. These trap packages were calibrated first by the NIST High Accuracy Cryogenic Radiometer at laser wavelengths of 633 nm and 442 nm. They were also measured in the NIST Spectral Comparator Facility with working standards traceable to a 100 % quantum efficient radiometer (QED-200). The two sets of measurements agree to better than 0,1 % at 633 nm and 0,25 % at 442 nm.

## 1. Introduction

Lower uncertainties in detector spectral calibrations are required as silicon photodiodes are applied to more demanding applications. Photodiodes are used singly or in combination with filters or other optical elements for responsivity, photometry, radiance and irradiance measurements. The Council for Optical Radiation Measurements, CORM, issued in its Fifth Report a list of the measurement uncertainty needs for national radiance and irradiance standards [1]. These goals, as well as others of the industrial, scientific and aerospace communities, depend on more accurate radiometric standards.

The NIST absolute spectral-responsivity scale for photodetectors is based on spectral-responsivity measurements of 100 % quantum-efficient silicon-photodiode light-trapping detectors, QED-200s, which serve as the primary standard [2, 3]. Single-photodiode working-standard detectors are calibrated against the QED-200s at the monochromator-based Spectral Comparator Facility (SCF). Routine calibrations are performed at this facility using the working standards. The total uncertainty of the spectral response scale, as maintained on the SCF, has been given as 0,33 % ( $3\sigma$ ) across the visible spectrum [2]. This must be reduced to meet present needs as described above. Improvement is being achieved by de-

veloping a more precise primary standard and the transfer devices needed to calibrate the working standards.

In this work, we demonstrate the NIST High Accuracy Cryogenic Radiometer (HACR) as a primary standard. We compare measurements of silicon photodiode trap detectors, using both the HACR and the present detector-response scale, at laser wavelengths of 633 nm and 442 nm. This is the initial step in the integration of the HACR into the detector absolute spectral response scale.

## 2. Detectors

### 2.1 High Accuracy Cryogenic Radiometer

The HACR operates as an Electrical Substitution Radiometer (ESR), a device that balances optical power with electrical power. Optical radiation is absorbed by, and heats, a receiving cavity. Electrical heating is then substituted for the optical power which gives the same temperature rise and is measured with instrumentation whose calibrations are based on NIST electrical standards.

Electrical substitution is a well-known technique for determining optical power [4]. While room-temperature ESR measurements can have uncertainties of 0,1 % or more, the technique can be more precise and accurate at cryogenic temperatures because of several favourable factors. The heat capacity of the

J. M. Houston, C. L. Cromer, J. E. Hardis and T. C. Larason:  
National Institute of Standards and Technology,  
Gaithersburg, MD 20899, USA.

receiving cavity material (copper) is much reduced, which leads to faster response times. The thermal conductivity of the cavity is increased, which leads to smaller temperature gradients and so reduces non-equivalence errors, that is, errors which depend on where the power is applied to the cavity. The cavity heater can be isolated from the surroundings by using thin, superconducting wires, reducing the uncertainty due to lead-heating. At low temperatures the radiative losses and their fluctuations are much reduced, and convective losses are not a factor because the cavity operates under high vacuum. However, the vacuum environment requires an entrance window for the optical radiation, which can cause additional measurement uncertainties. Since its transmittance is not precisely unity a correction factor must be applied, and its temperature must be sufficiently stable not to change significantly the background radiation received by the cavity.

The NIST radiometer, shown in Figure 1, is based on the NPL design [5]. Laser radiation enters through the window at the bottom and travels through apertures and two alignment photodiodes to the absorbing cavity in the middle. The beam is collimated to a diameter of less than 6 mm in order

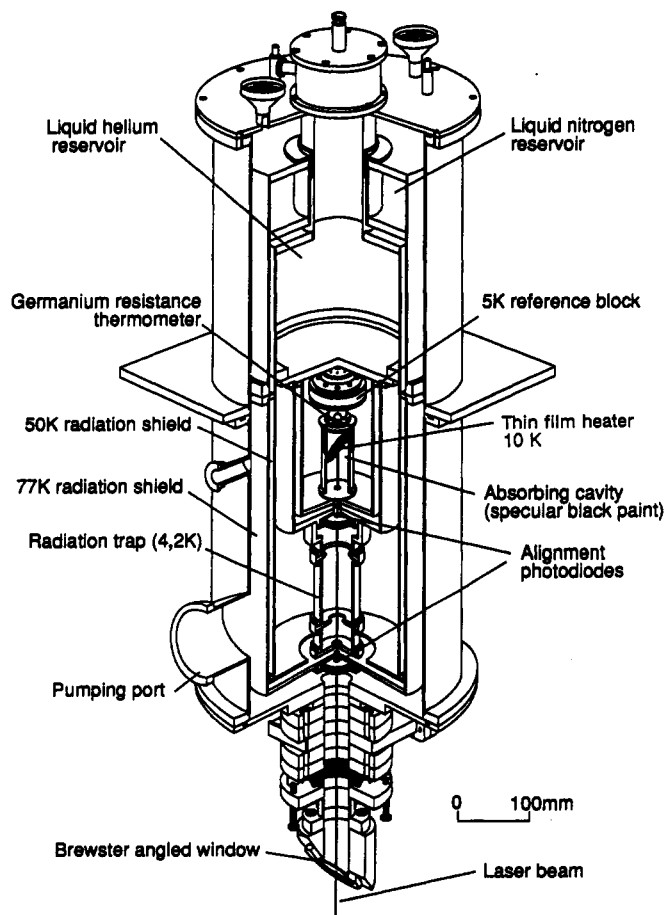


Figure 1. The High Accuracy Cryogenic Radiometer.

to pass through the apertures with less than 0,01 % loss.

The cavity is a copper cylinder, 150 mm in length and 50 mm in diameter, with an internal baffle at 30° that traps the incident laser beam with multiple reflections. Its interior is painted with specular black paint. We determined the absorbance of the cavity by measuring its diffuse reflectance relative to a NIST polytetrafluoroethylene (PTFE) reflectance standard. Using a 632,8 nm HeNe laser beam as the source, the cavity absorbance was 99,998 %.

The cavity is attached to an actively stabilized 5 K reference block through a low-conductance heat link. Regulation of the block temperature isolates the cavity from thermal fluctuations of the cryostats and maintains a correspondence between the cavity temperature and the applied power. With this heat link, 1 mW of input power causes the cavity temperature to rise approximately 1 K above the block temperature. (The niobium wires on the cavity heater are only superconducting below 9,7 K, the operational limit.) The temperatures of both the cavity and block are monitored with germanium resistance thermometers (GeRTs).

## 2.2 Transfer devices: silicon photodiode light-trapping detectors

Detectors calibrated against the HACR can transfer accuracy to various radiometric endeavours, provided that they are carefully chosen for the purpose. Ideally the transfer detectors would have a precision comparable with the HACR, long-term stability (including insensitivity to temperature changes and other environmental influences), and a dynamic range that spans both the power level required for the HACR and the power level of the target application.

For this work, we used windowless Hamamatsu S1337-1010BQ photodiodes arranged in a light-trapping configuration. A photodiode light-trap is an arrangement whereby the optical radiation reflected by a photodiode is intercepted by other photodiodes, as shown in Figure 2. The combination produces more complete absorption than is possible with an individual photodiode. With three photodiodes and five reflections, the overall absorption is greater than 99,9 % at visible wavelengths. The responsivities of light-trapping packages are also more spatially uniform and insensitive to surface changes (such as those caused by adsorption of atmospheric water) than individual photodiodes. Additionally, the photodiodes are rotated in different planes to minimize the polarization sensitivity. This is important because the light-trap may be used with sources having different degrees of polarization.

Among the differences between our own light-trap configuration and the QED-200 design is that

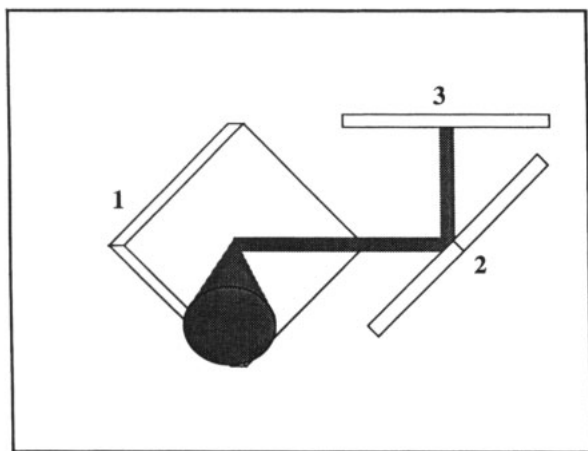


**Figure 2.** Layout of light-trapping silicon-photodiode detector. The arrangement of the photodiodes reduces the light lost to reflection.

we used Hamamatsu 1337 P-on-N junction devices. For this application, 100 % internal quantum efficiency was unnecessary. Also, the 1337s have a higher response at red wavelengths. Measurements of single 1337s show that temperature affects the responsivity by less than 0,02 %/°C from 400 nm to 950 nm, and that deviations from linearity are less than 0,01 % in the photocurrent range  $10^{-4}$  A to  $10^{-9}$  A. The long-term stability of these light-traps is better than 0,04 % at 633 nm over a period of ten months.

### 3. Measurements

#### 3.1 HACR measurements

A HACR calibration of a light-trapping detector comprises three steps: the laser heating of the HACR cavity, the electrical heating of the HACR cavity to the same temperature, and the detector measurement of the same laser power. For the present work, the laser beam was prepared and directed into the HACR as shown in Figure 3. The beam was intensity-stabilized in order to maintain the same power for the HACR and detector measurements, using a commercial electro-optic stabilizer and a remote monitor photodiode. Between the stabilizer and the wedged beam-splitter additional elements, a spatial filter, lens and aperture, removed divergent modes from the beam and focused it into the HACR. A final aperture blocked stray radiation.

When optical or electrical power was applied to the HACR cavity, its temperature approached a new thermal equilibrium. The voltage across the cavity GeRT, powered at constant current, was sampled at approximately 1 Hz by a data-acquisition computer system. The computer display showed the series of

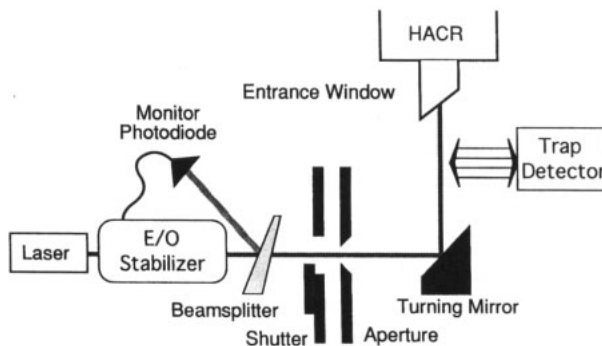


**Figure 3.** Laser source for HACR calibrations.

voltages, and the mean and standard deviation of the most recent 100 measurements. An equilibrium temperature was considered to have been reached when (a) the standard deviation was less than 0,006 % of the mean, and (b) the mean for the 633 nm wavelength was stable to within 0,001 % over a 5 min period. (At 442 nm, a stability of only 0,003 % was obtained due to the greater noise at lower laser power.) These conditions were usually met within 45 min after initiation of the electrical or optical heating.

Electrical heating of the cavity was performed twice, once with an equilibrium temperature slightly above the optically induced temperature, and once with an equilibrium slightly below it. The laser power was calculated by linearly interpolating between these two heater measurements. At the beginning of the first heating cycle, while waiting for equilibrium to be reached, the laser power was applied to the light-trapping detector. This measurement was completed within 5 min.

The electrical substitution balances only the optical radiation that is absorbed by the cavity. Some of the radiation is lost due to scatter of the beam, window effects and reflection from the cavity, so corrections to the electrical power measurement need to be applied to deduce the actual laser power.

A power correction calculated from the small, residual signal of the alignment photodiodes was added to the heater power. This signal was caused mostly by scattered light, such as from imperfections on the turning mirror and the entrance window. Additionally, the entrance window absorbed and reflected less than 0,05 % of the laser beam, even at the optimum angle. Its transmittance was measured at the same angle for each wavelength, when separate from the vacuum system. This factor and the cavity reflectance of 99,998 % were used to correct for the losses.

#### 3.2 Monochromator measurements

The light-trapping detectors calibrated by the HACR were also calibrated at the SCF. Their absolute spectral responsivities were measured over the wavelength

range 350 nm to 1 100 nm, in 5 nm steps, by comparison with the working standards. The spectral responsivities of the light-trapping detectors at 442 nm and 633 nm were determined by linear interpolation of the neighbouring wavelengths. The external quantum efficiencies of the light-trapping detectors were calculated from the spectral response measurements.

The SCF uses a prism-grating monochromator with a bandpass of 4 nm and stray-light rejection of  $10^{-8}$  [6]. A quartz-halogen lamp was focused onto the 1,1 mm entrance slit of the monochromator, which projected a 1,1 mm, nearly circular, spot onto the detector under test. Variations in the source intensity were corrected by using a beam-splitter and monitor detector. The instrument can align, move, and spectrally scan the detectors under computer control.

#### 4. Results

The external quantum efficiencies of two light-trapping detectors, as computed from the measured spectral responsivities using the two methods, are shown

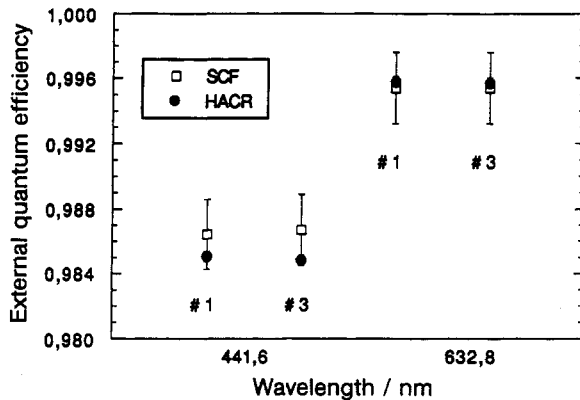


**Figure 4.** The external quantum efficiency with expanded uncertainties ( $2\sigma$ ) of two light-trapping detectors, as measured at two wavelengths by the HACR and the SCF.

in Figure 4. The HACR values are based on the averages of at least six independent laser power measurements, while the SCF values are the average of three independent runs. Tables 1 and 2 show the agreement between these two data sets to be better than 0,1 % at 633 nm and 0,25 % at 442 nm.

The SCF was also used to measure the response uniformity of the active areas of the light-trapping detectors at 500 nm. They were mapped by moving them across the monochromator spot in 0,5 mm steps. Figure 5 shows the mapping of a typical light-trapping detector, indicated as #3 in Figure 4. Outwards from the centre, each contour indicates a drop in responsivity by 0,01 % of the maximum value. The responsivity plateau is only  $\sim 2$  mm on a side

**Table 1.** Comparison of the SCF and the HACR external quantum efficiencies at 442 nm.

Trap number	External quantum efficiency		Difference $\times 10^2$
	SCF	HACR	
HMT # 1	0,986 43	0,984 80	-0,17
HMT # 3	0,986 71	0,984 55	-0,22

**Table 2.** Comparison of the SCF and the HACR external quantum efficiencies at 633 nm.

Trap number	External quantum efficiency		Difference $\times 10^2$
	SCF	HACR	
HMT # 1	0,995 40	0,995 77	0,04
HMT # 3	0,995 40	0,995 69	0,03

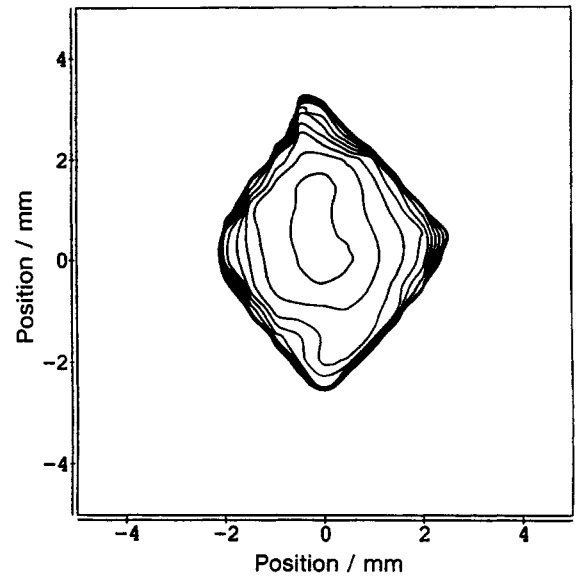


**Figure 5.** Uniformity map of light-trapping silicon-photodiode detector #3 at 500 nm. Each contour from the centre indicates a drop in responsivity of 0,01 %.

because of the limited depth of field of the focused SCF spot. Nevertheless, it is clear that positional differences can modify the responsivity by amounts of order 0,03 %, even when an effort is made to maximize the signal while aligning the light-trapping detector in a laser beam.

The uncertainty bars in Figure 4 show the total calibration ( $2\sigma$ ) uncertainties for the HACR and the SCF. The uncertainty budgets are itemized in Tables 3 and 4, respectively. The SCF uncertainties in Table 4 are discussed in [2]: by far the largest

**Table 3.** Measurement uncertainties for the HACR and trap. Uncertainties are expressed in terms of the standard deviation  $\sigma(y)$  of the mean values  $y$  of the contributing factors listed. Correction factors for window transmission are also listed. The total uncertainty is 0,0133 % at a wavelength of 633 nm and 0,03 % at a wavelength of 442 nm.

Contributing factors	633 nm		442 nm	
	$10^4 \times \sigma(y)/y$	Correction factor	$10^4 \times \sigma(y)/y$	Correction factor
<b>Transmission errors</b>				
Window transmittance	0,33	1,000 2	0,33	1,000 2
Scatter	0,17	1,000 09	0,17	1,000 2
Cavity absorptance	0,2	1,000 02	0,2	1,000 02
<b>Electrical power measurement errors</b>				
Voltage measurement of the heater and standard resistor	0,33		0,33	
Resistance of standard resistor	0,033		0,033	
<b>Power equivalence errors</b>				
Cavity thermal gradients	*		*	
<b>Reproducibility</b>				
Balance determination	0,7		2	
Trap positioning	1,0		1	
Other			2	
Sum in quadrature	13,3		3	

\* This value is expected to be small.

**Table 4.** Measurement uncertainties for the SCF. Uncertainties are expressed in terms of the standard deviation  $\sigma(y)$  of the mean values  $y$  of the contributing factors listed. The total uncertainty is 0,114 %.

Contributing factors	$10^4 \times \sigma(y)/y$
Detector nonuniformity	1
Random noise on the SCF	3
Detector scale basis uncertainty	11
Sum in quadrature	11,4

contribution is the present scale basis. The largest contributions to the measurement uncertainty of a HACR calibration arise from failures of reproducibility. The process of temperature measurement contributed to this, both through the noise of the GeRT circuits and through the long wait for three temperature equilibria to be reached. The variation of the temperature data leads to a standard uncertainty in power of 0,007 % at 633 nm and 0,02 % at 442 nm. A standard uncertainty of 0,01 % was associated with removing and repositioning a light-trapping detector, perhaps due to the difficulty of aligning the detector consistently. Other effects include the performance of the laser stabilizer and the compromise of beam quality at 442 nm in order to obtain sufficient operating power. This will be described in a subsequent paper. Overall, the reproducibility had a standard deviation of about 0,012 % for the 633 nm data, and 0,03 % for the 442 nm data.

## 5. Conclusion

The light-trapping detector measurements by the HACR and the SCF are the first step toward shifting the base of the detector absolute spectral response scale to the cryogenic radiometer. Calibrations by these methods agree within their standard uncertainties. However, the advantage of basing the scale on the cryogenic radiometer is that the scale standard uncertainty can be reduced by using automation and improved measurement systems, potentially from 0,11 % to 0,0033 % ( $1\sigma$ ).

Subsequent to this work, we have further automated the HACR, which has led to better measurement reproducibility and faster operations. This work continues, along with efforts to reduce the various noise sources that affect the result. Nevertheless, the nonuniformities of the light-trapping detectors remain at 0,02 % to 0,03 % across their active area. Until a more uniform transfer device is developed, the trap-detector nonuniformities will remain a limitation to the HACR calibration transfer.

**Note:** Certain commercial equipment, instruments, or materials are identified in this paper in order to specify the experimental procedure adequately. Such identification is not intended to imply recommendation or endorsement by the National Institute of Standards and Technology, nor is it intended to imply

that the materials or equipment identified are necessarily the best available for the purpose.

**Acknowledgements.** Much credit in the success of this project goes to Joel Fowler, whose skill made the HACR operational, to Al Parr, who recognized early the value of cryogenic radiometry and who consistently provided his advice and support, and to Steve Southworth, who made preparations for the NIST instrument. The authors offer special thanks to Nigel Fox and David Nettleton of the NPL, whose hospitality and assistance is greatly appreciated.

## References

1. *CORM Fifth Report: Pressing Problems and Projected National Needs in Optical Radiation Measurements*, Council for Optical Radiation Measurements, September 1989.
2. Cromer C. L., A New Spectral Response Calibration Method using a Silicon Photodiode Trap Detector, to be published.
3. Zalewski E. F., Duda C. R., Silicon photodiode device with 100 % external quantum efficiency, *Appl. Opt.*, 1983, **22**, 2867-2873.
4. *Absolute Radiometry: Electrically Calibrated Thermal Detectors of Optical Radiation*, (Edited by F. Hengstberger), San Diego, Academic Press, 1989.
5. Martin J. E., Fox N. P., Key P. J., A Cryogenic Radiometer for Absolute Radiometric Measurements, *Metrologia*, 1985, **21**, 147-155.
6. Saunders R. D., Shumaker J. B., Apparatus function of a prism-grating double monochromator, *Appl. Opt.*, 1986, **25**, 3710-3714.